Analysis of Dust and Fission Products in PBMR Turbine

M.M. Stempniewicz, NRG Arnhem, Utrechtseweg 310, P.O.Box 9034 6800 ES Arnhem, The Netherlands

D. Wessels, PBMR, 1279 Mike Crawford Avenue, Centurion 0046, Republic of South Africa

ABSTRACT

A 400 MWth direct cycle Pebble Bed Modular reactor was under development in South Africa. The work performed included design and safety analyses. In HTR/PBMR, graphite dust is generated during normal reactor operation due to pebble-to-pebble scratching. This dust will be deposited throughout the primary system. Furthermore, the dust will become radioactive due to sorption of fission products released, although in very small quantities, during normal operation. This paper presents a model and analyses of the PBMR turbine with the SPECTRA code. The purpose of the present work was to estimate the amount and distribution of deposited dust and the fission products, namely cesium, iodine, and silver, during plant life-time, which was assumed to be 40 full-power years.

The performed work showed that after 40 years of plant life-time deposited layers are very small. The largest deposition is of course observed on the dust filters. Apart from the dust filters, the largest dust deposition is observed on the:

- Outer Casing (inner walls)
- Turbine Rotor Cooling Cavity (inner walls)
- HPC Cold Cooling Gas Header (inner walls)

This is caused by relatively low gas velocities in these volumes. The low velocities allow a continuous build-up of the dust layer.

About 90% of cesium, 40% of iodine, and 99.9% of silver is adsorbed on the metallic structures of the turbine. The sorption rate increases along the turbine due to decreasing temperatures. In case of cesium and iodine the highest concentrations are observed in the last stage (stage 12) of the turbine. In the case of silver the sorption is so large that the silver vapor is significantly depleted in the last stages of the turbine. This is a reason for having a maximum in silver concentration in the stage 10. In the following stages the concentration decreases due to very small silver vapor fraction in the gas.

1 Introduction

A 400 MWth direct cycle Pebble Bed Modular reactor was under development in South Africa. The work performed included design and safety analyses. In HTR/PBMR, graphite dust is generated during normal reactor operation due to pebble-to-pebble scratching. This dust will be deposited throughout the primary system. Furthermore, the dust will become radioactive due to sorption of fission products released, although in very small quantities, during normal operation. This paper presents a model and analyses of the PBMR turbine with the SPECTRA code. The purpose of the present work was to estimate the amount and distribution of deposited dust and the fission products, namely cesium, iodine, and silver, during plant life-time, which was assumed to be 40 full-power years.

A model of the PBMR turbine for plateout analyses with the SPECTRA code [1] has been prepared in cooperation between PBMR (South Africa) and Nuclear Research and Consultancy Group (NRG) based on the data available from references [2], [3], [4], [5]. The model has been applied:

- to perform a long term (plant life-time) analysis of dust transport,
- to perform a long term (plant life-time) analysis of fission product transport and plateout.

The turbine model is shortly presented in section 2. Section 3 presents results of calculations performed with the model. Finally, section 4 presents conclusions and recommendations.

2 SPECTRA model of PBMR Turbine

2.1 SPECTRA Code

The SPECTRA code [1] is an accident analysis code developed at NRG, the Netherlands. SPECTRA (Sophisticated Plant Evaluation Code for Thermal-hydraulic Response Assessment) is a computer program designed for thermal-hydraulic analyses of nuclear or conventional power plants.

Within the part of the code called Radioactive Particle Transport Package (RT Package) models are available for release of fission products, aerosol transport, deposition, and resuspension. Radioactive chains of fission products are tracked. The following aerosol models are available in the SPECTRA code:

- Gravitational settling
- Thermophoresis
- Brownian diffusion
- Turbulent deposition
- Inertial impaction
- Resuspension
- Coagulation (agglomeration) of aerosol particles and deposited particles
- Inter-volume aerosol transport

The following fission product models are included in the SPECTRA code:

- FP release models (CORSOR, CORSOR-M, user-defined functions)
- Condensation of FP Vapors.
- Sorption of FP vapors on surfaces, on aerosol particles and deposited particles. Two sorption models are available:
    - Sorption Model 1 (SPECTRA model). A simpler model, similar to the one adopted in the MELCOR code [10], developed by Sandia.
    - Sorption Model 2 (PATRAS/SPATRA model). A more detailed model adopted for the codes PATRAS, SPATRA [11], [12], developed at Jülich.

An extensive Verification and Validation (V&V) of the code has been performed using measured data as well as code to code comparisons for various types of power plants. The V&V related to HTR's, in particular sorption of fission product vapors, consists of AVR data; Laminar Loop experiments, Vampyr and Dragon experiments. The V&V is described in detail in Volume 4 of reference [1].

2.2 Nodalization

The turbine model has been developed at PBMR based on system drawings and turbine maps and efficiency data for each turbine stage, references [2], [3], [4], [5]. Nodalization diagrams of the PBMR Turbine model are shown in Figure 1, Figure 2, and Figure 3. The figures can be generally described as:

- Connections, Figure 1, shows all cooling lines and connections at the boundaries.
- Main body, Figure 2, shows the turbine with all internal cooling flows and leak flows.
- Stages, Figure 3, shows the performance of turbine stages, power per stage, rotor and stator cooling flow per stage.

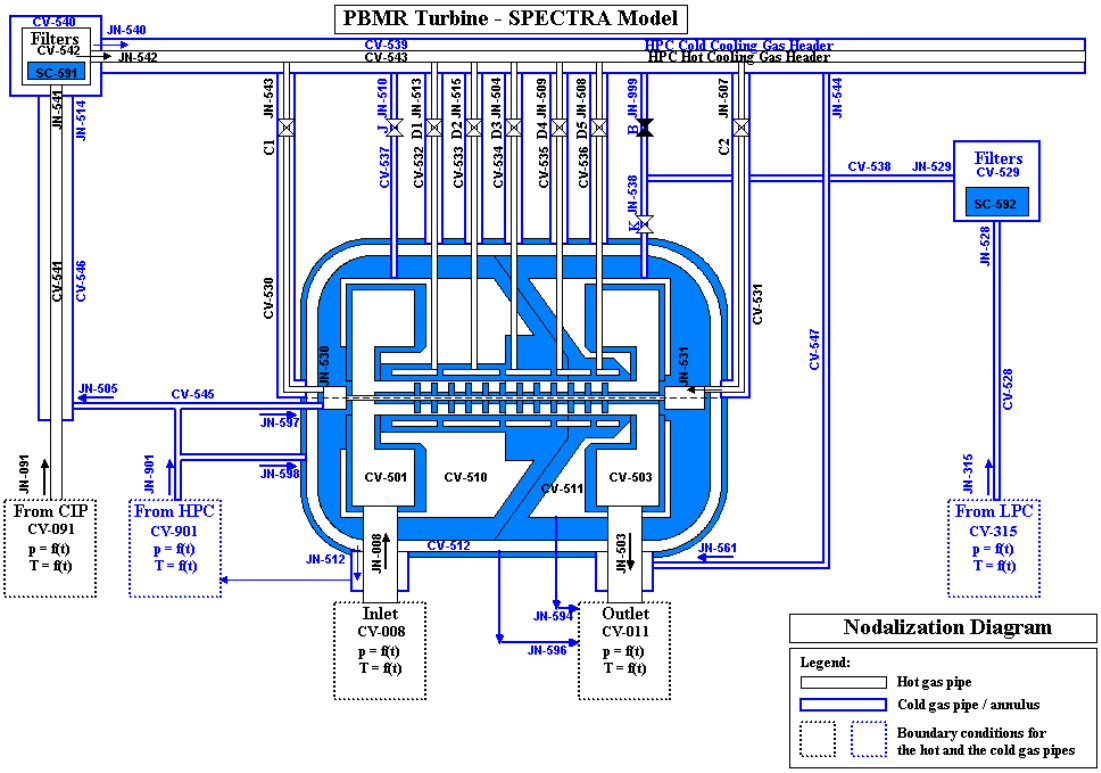

Figure 1 Turbine - connections

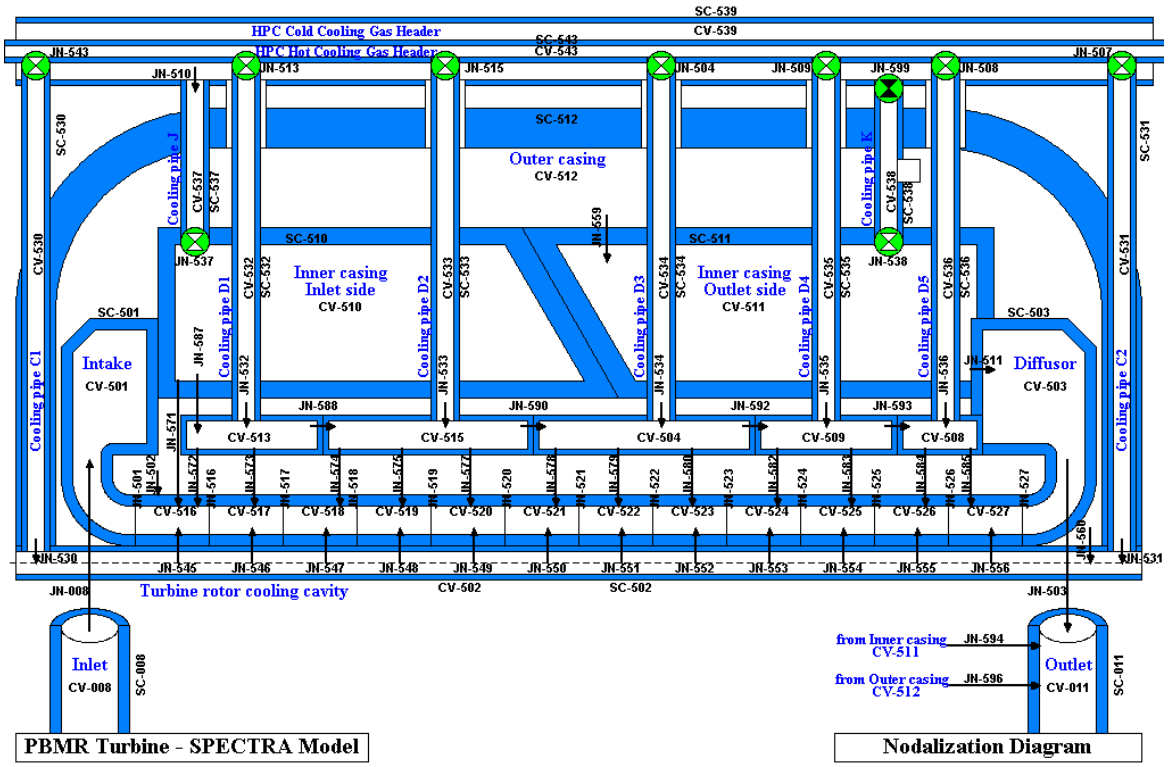

Figure 2 Turbine - main body

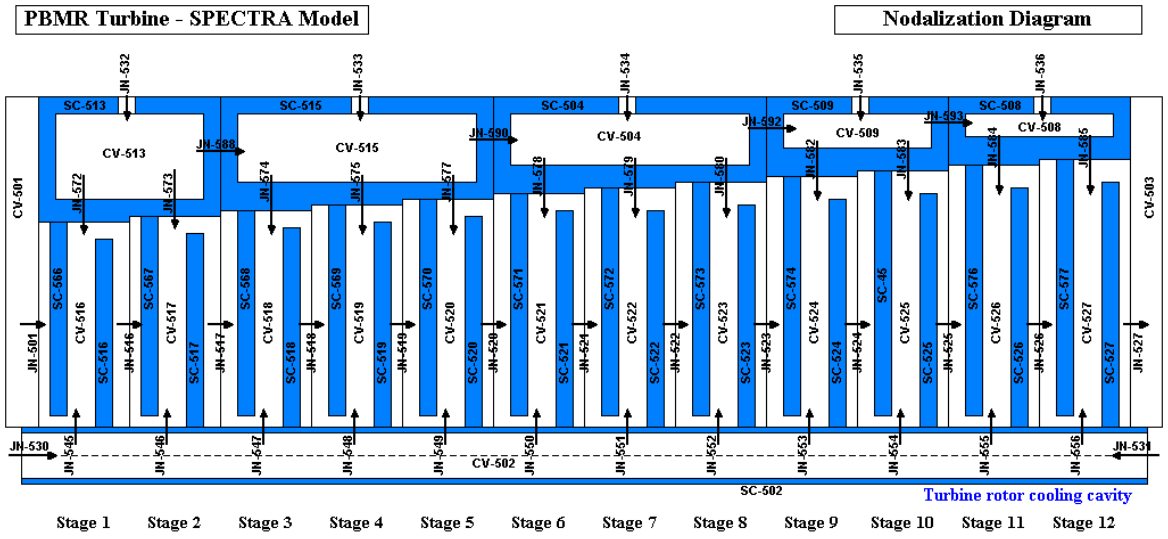

Figure 3 Turbine - stages

The model consists of 47 Control Volumes (CV), 85 Junctions (JN), and 58 1-D Solid Heat Conductors (SC). Each of the 12 stages of the turbine has been modeled explicitly using a Turbine Junction, available in SPECTRA [1], with the turbine maps and stage efficiency supplied based on available data [2], [5].

The model has five boundaries, for which the boundary conditions must be supplied (Figure 1):

- Turbine inlet (CV-008)
- Turbine outlet (CV-011)

- Inlet from Core Inlet Pipe (CIP) to the Hot Cooling Gas Header (CV-091)
- Inlet from High Pressure Compressor (HPC) to the Cold Cooling Gas Header (CV-901)
- Inlet from Low Pressure Compressor (LPC) to the turbine inner casing (CV-315)

The boundary conditions are taken from available design data or calculations performed with a full model.

The model has been tested by performing a run fat 100% power and comparing the main parameters, such as flows, pressures, temperatures, to the design data from Mitsubishi [3] and the values obtained with the Flownex code [4]. The flow resistance factors of the leak flows paths and the cooling lines have been adjusted to match the flows in agreement with the design data. The model and test calculations are described in reference [6] and is not further discussed here. The modeling assumptions and data related to the dust and fission products are described below.

2.3 Dust Models

To perform the dust and fission product analyses the Radioactive Particle Transport Package (RT) in SPECTRA was activated and the following input coefficients were selected:

- Density of dust particles: 1750.0 [kg/m^3]
- Thermal conductivity of dust particles: 10.0 [W/(m-K)]
- Porosity of deposited layers: 0.5 [-]

Fifteen dust size sections were used, the same as used for PBMR and NGNP analyses. The size sections representative diameters are listed in Table 1.

Table 1 Diameters of dust size sections

Size sec.	1	2	3	4	5
D, [m]	0.202E-6	0.353E-6	0.493E-6	0.632E-6	0.873E-6
Size sec.	6	7	8	9	10
D, [m]	1.218E-6	1.598E-6	1.953E-6	2.322E-6	2.718E-6
Size sec.	11	12	13	14	15
D, [m]	3.078E-6	3.458E-6	10.00E-6	20.00E-6	50.00E-6

The resuspension model of Vainshtein was used, with “all defaults” and the following input parameters for the adhesion force calculation:

- Surface roughness: 10^{-5} [m]
- Relative humidity 1.0 [-]

The dust filters were modeled using the inertial impaction model with impaction efficiency equal to the dust filter efficiency: 0.9. The filter efficiency was estimated by experts from PBMR as exact value was not known. The model was activated on the dust filter structures: SC-591 and SC-592. The inertial impaction model for these structures was associated with the jet from the inlet junctions: JN-514 and JN-528 respectively (Figure 1). The inertial impaction model was used instead of the aerosol filter model because in SPECTRA a filter is associated with junction (JN) and no sorption model exists for dust particles present in JN. In order to be able to calculate sorption on dust present on the filter, the filter must be represented by a solid structure (SC), since the sorption of fission products on SC-deposited particles is calculated by the code.

2.4 Fission Product Models

- For the metallic surfaces, the Sorption Model 2 (PATRAS/SPATRA model) available in SPECTRA [1] was applied:

$$S_{total} = \alpha \cdot (1-\theta) \cdot u \cdot C_{\delta} - \vartheta \cdot C_{rev} - \eta \cdot C_d$$
$$S_{diff} = \alpha \cdot (1-\theta) \cdot u \cdot C_{\delta} \cdot (1-\beta) - \eta \cdot C_d$$

Here S_{total} is the total sorption flux [kg/s], S_{diff} is the part that penetrates and diffuses into the material [kg/s], α is the sticking coefficient (assumed =1.0), θ is reversible surface coverage, C_{δ} is the vapor concentration in the δ-sublayer, [kg/m^3], C_{rev} is the number of adsorption sites occupied by reversibly bound molecules per unit surface area, [m^{-2}], ϑ is the desorption coefficient, [s^{-1}], η is the evaporation coefficient, [s^{-1}] (assumed =0.0), and $(1-\beta)$ is the penetration factor. The coefficients ϑ, $(1-\beta)$, $(1-\theta)$ are given by:

$$\vartheta = \vartheta_0 \cdot \exp\left(-\frac{A_{\vartheta}}{T_w}\right)$$
$$(1-\beta) = (1-\beta_0) \cdot \exp\left(\frac{A_{\beta}}{T_w}\right)$$
$$(1-\theta) = \left(1-\frac{C_{rev}}{C_{\max}}\right)$$

Here T_w is the wall temperature [K], $C_{\max}$ is the maximum number of sorption sites per unit surface area, [m^{-2}] (assumed equal to 4×10^{18}). The sorption parameters on metallic surfaces were assumed following [9]:

- Vapor class: Cs: $(1-\beta)=10^{-5}$, $\upsilon=10^{11}\exp(-28150/T)$, $\eta=0.0$
- Vapor class: I: $(1-\beta)=0.0$, $\upsilon=10^{11}\exp(-21666/T)$, $\eta=0.0$
- Vapor class: Ag: $(1-\beta)=10^{-5}$, $\upsilon=10^{11}\exp(-30670/T)$, $\eta=0.0$

- For the dust particles, the Sorption Model 1 (SPECTRA model) [1] was applied:

$$S = A(T) \cdot C_V - B(T) \cdot C_d$$

Here S is the sorption flux, C_V is the isotope concentration in the gas [kg/m^3], C_d is the isotope concentration on the surface [kg/m^2], $A(T)$ and $B(T)$ are temperature-dependent coefficients.

The following sorption coefficients on dust particles were assumed [8]:

- Cesium on dust.

$$A_S(T_w) = \begin{cases} 1.0 & for\ T = 500\ K \\ 1.0\times10^{-2} & for\ T = 800\ K \\ 1.0\times10^{-4} & for\ T = 1100\ K \end{cases}$$
$$B_S(T_w) = 1.0\times10^{-6}$$
$$C_{sat}(T_w) = \begin{cases} 1.0\times10^{-12} & for\ T = 500\ K \\ 1.0\times10^{-10} & for\ T = 800\ K \\ 1.0\times10^{-8} & for\ T = 1100\ K) \end{cases}$$

- Iodine on dust.

$$A_S(T_w) = \begin{cases} 4.5\times10^{-1} & for\ T = 500\ K \\ 4.5\times10^{-3} & for\ T = 800\ K \\ 4.5\times10^{-5} & for\ T = 1100\ K \end{cases}$$

$$B_S(T_w) = 1.0\times10^{-6}$$

$$C_{sat}(T_w) = \begin{cases} 4.0\times10^{-12} & for\ T = 500\ K \\ 4.0\times10^{-10} & for\ T = 800\ K \\ 4.0\times10^{-8} & for\ T = 1100\ K \end{cases}$$

- Silver on dust:

$$A_S(T_w) = \begin{cases} 1.0 & for\ T = 500\ K \\ 1.0\times10^{-2} & for\ T = 800\ K \\ 1.0\times10^{-4} & for\ T = 1100\ K \end{cases}$$

$$B_S(T_w) = 1.0\times10^{-6}$$

$$C_{sat}(T_w) = \begin{cases} 1.0\times10^{-12} & for\ T = 500\ K \\ 1.0\times10^{-10} & for\ T = 800\ K \\ 1.0\times10^{-8} & for\ T = 1100\ K) \end{cases}$$

3 Results

As a first step the turbine start up to a 100% power has been calculated and the thermal-hydraulic results were compared to the source data. The resulting temperatures and flows are shown in Figure 4. Accuracy of the thermal-hydraulic solution is discussed in [6] and is considered sufficient for the dust and fission product analyses.

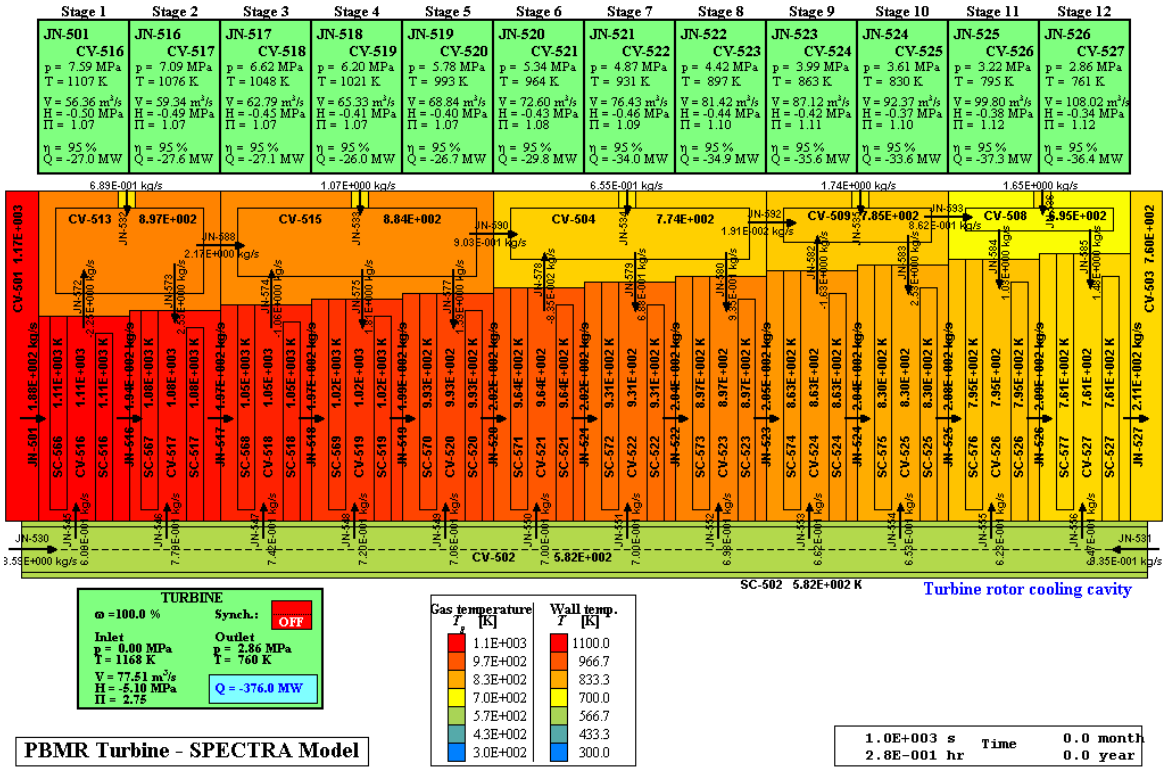

Figure 4 Turbine stages data, pressures, temperatures, flows

Two runs are presented below:

- Long-term dust analysis for the turbine at 100% power - discussed in section 3.1.
- Long-term analysis of fission products for the turbine at 100% power - discussed in section 3.2.

3.1 Long-Term Dust Analysis for the Turbine at 100% Power

The purpose of this run is to investigate dust transport and deposition on the turbine structures during the plant life-time. The plant life-time of 40 years was assumed.

The dust concentrations at the turbine boundaries were assumed based on the values calculated for the NGNP plant [7]. This was done in absence of full model PBMR results. The airborne dust concentrations at the outlet of the NGNP reactor vessel (CV-510) were used. The dust masses for

each size section in the NGNP outlet pipe are listed in Table 2. The values listed in Table 2 were used at the following boundaries:

- CV-008 (inlet)
- CV-315 (LPC)
- CV-901 (HPC)
- CV-091 (CIP)

Table 2 Dust concentrations at the turbine boundaries

Size sec.	1	2	3	4	5
Mass [kg]	8.19231E-10	1.49819E-08	8.85027E-08	1.09654E-07	1.22373E-07
Size sec.	6	7	8	9	10
Mass [kg]	2.39009E-07	1.85693E-07	1.49783E-07	1.17983E-07	9.02195E-08
Size sec.	11	12	13	14	15
Mass [kg]	4.84947E-08	1.43496E-07	1.86656E-10	7.38372E-08	1.57060E-07

Results are shown in Figure 5, Figure 6, Figure 7, and Figure 8. The figures show:

- Airborne dust concentrations (sum of all size sections) in Control Volumes in [$1/m^3$], shown using the grey scale.
- Deposited layer thickness (calculated using the assumed porosity of the dust layer of 0.5) on the surfaces of Solid Heat Conductors in [m], shown using the triple, blue-yellow-red, color scale.

The airborne concentrations in the main stream decrease to about half of the inlet value (from 2.25×10^8 m^{-3} in the intake to 1.06×10^8 m^{-3} in the diffusor). This is an effect of gas decompression. Due to decompression the same mass of gas occupies larger volume and consequently the same mass of dust occupies larger volume. Therefore the gas concentrations, expressed in particles per unit volume are decreasing. The decrease of dust concentrations along the main stream has nothing to do with deposition on the turbine structures, which, as will be shown below, is very small in the turbine main stream. This is seen in Figure 6 as the dust flow at the inlet (8.94E-6 kg/s) and at the outlet (9.21E-6 kg/s) are very similar. A small increase in the dust flow is caused by dust entering the main stream through the cooling lines.

After 40 years of plant life-time deposited layers are very small (of order of 10^{-5} m on the stator and rotor blades - Figure 7). The largest deposition is of course observed on the dust filters (Figure 5). Apart from the dust filters, the largest dust deposition is observed on (Figure 6):

- Outer Casing (inner walls) 2.48×10^{-4} m
- Turbine Rotor Cooling Cavity (inner walls) 2.30×10^{-4} m
- HPC Cold Cooling Gas Header (inner walls) 1.58×10^{-4} m

This is caused by relatively low gas velocities in these volumes (the values are about 0.15, 0.10, and 5 m/s in these three volumes respectively). There is a continuous build-up of the dust layer in the regions because the gas valocities are too low to cause any significant dust resuspension. In other places of the system the dust is resuspended very quickly due to large gas velocities, and an equilibrium layer develops. The equilibrium layer thickness is a result of coagulation of the deposited dust; as the larger particles are quickly resuspended. Figure 8 shows the deposited layer thicknesses in the three surfaces with the largest deposition, and the layer thickness on the stator

of the Stage 1. It is seen that an equilibrium layer on the stator develops very quickly. The same behavior is observed on all stator and rotor structures and therefore the net deposition rate on these structures is practically zero.

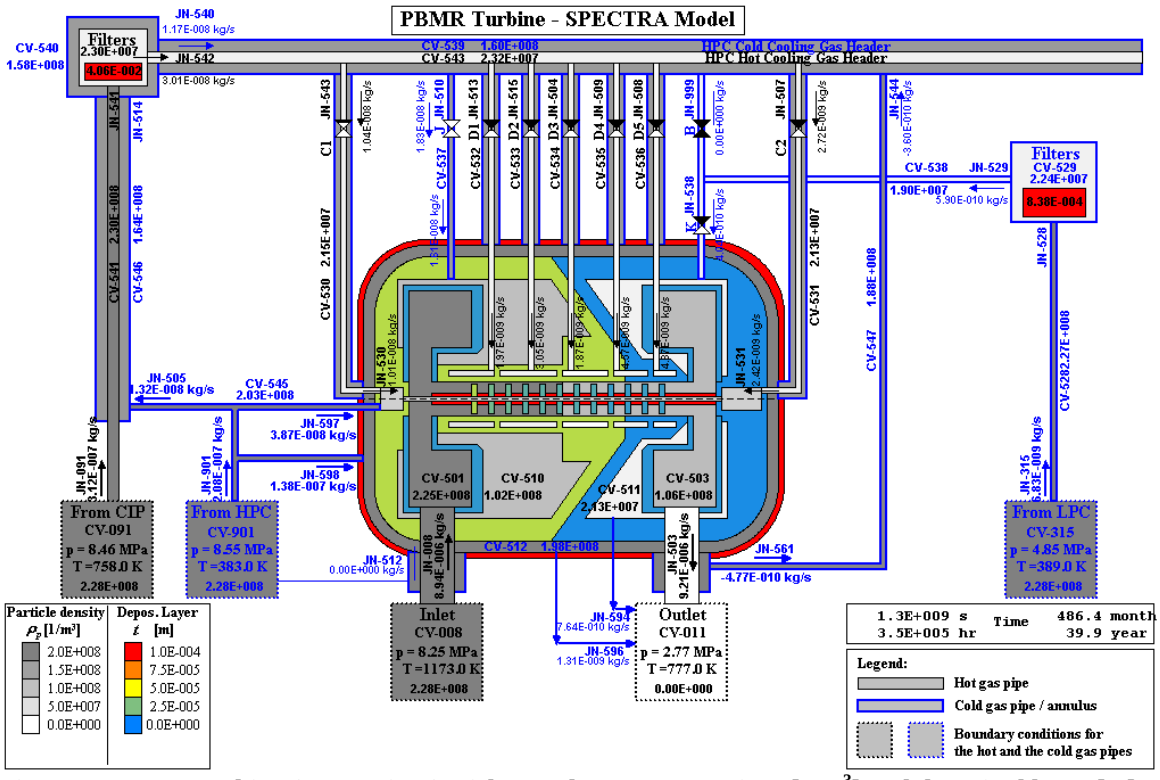

Figure 5 Turbine (connections), airborne dust concentrations [1/m^3] and deposited layer [m]

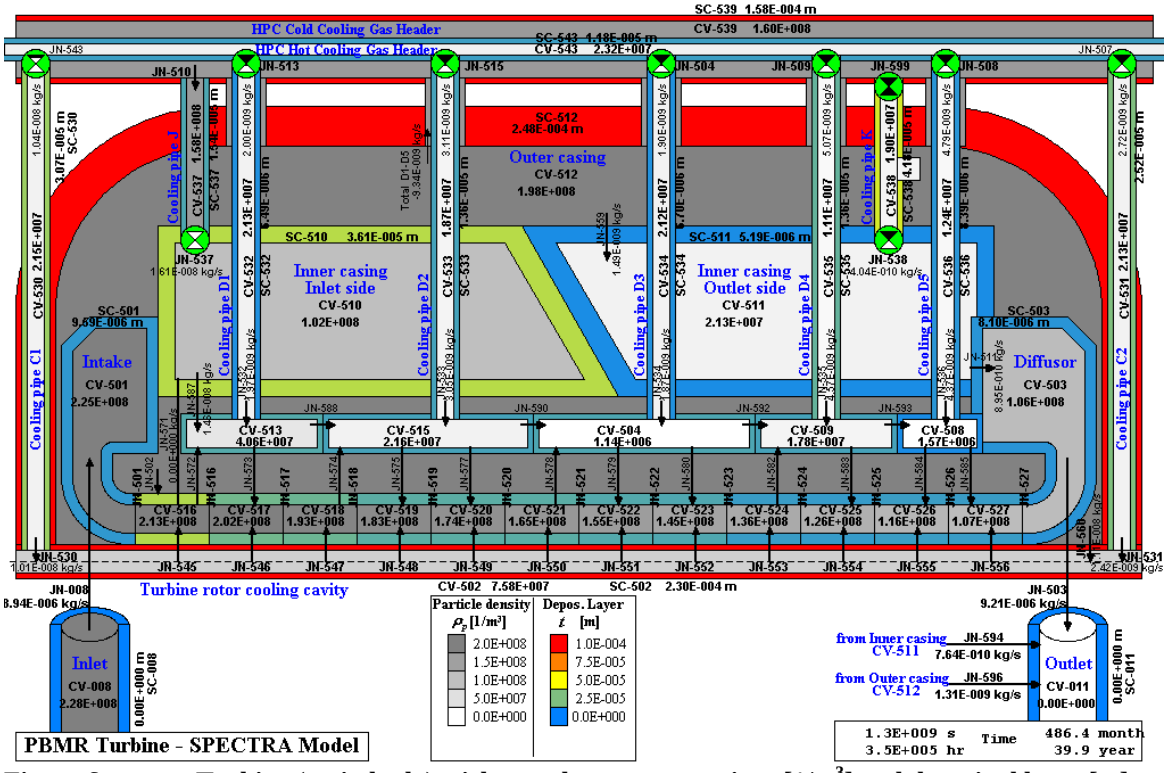

Figure 6 Turbine (main body), airborne dust concentrations [1/m^3] and deposited layer [m]

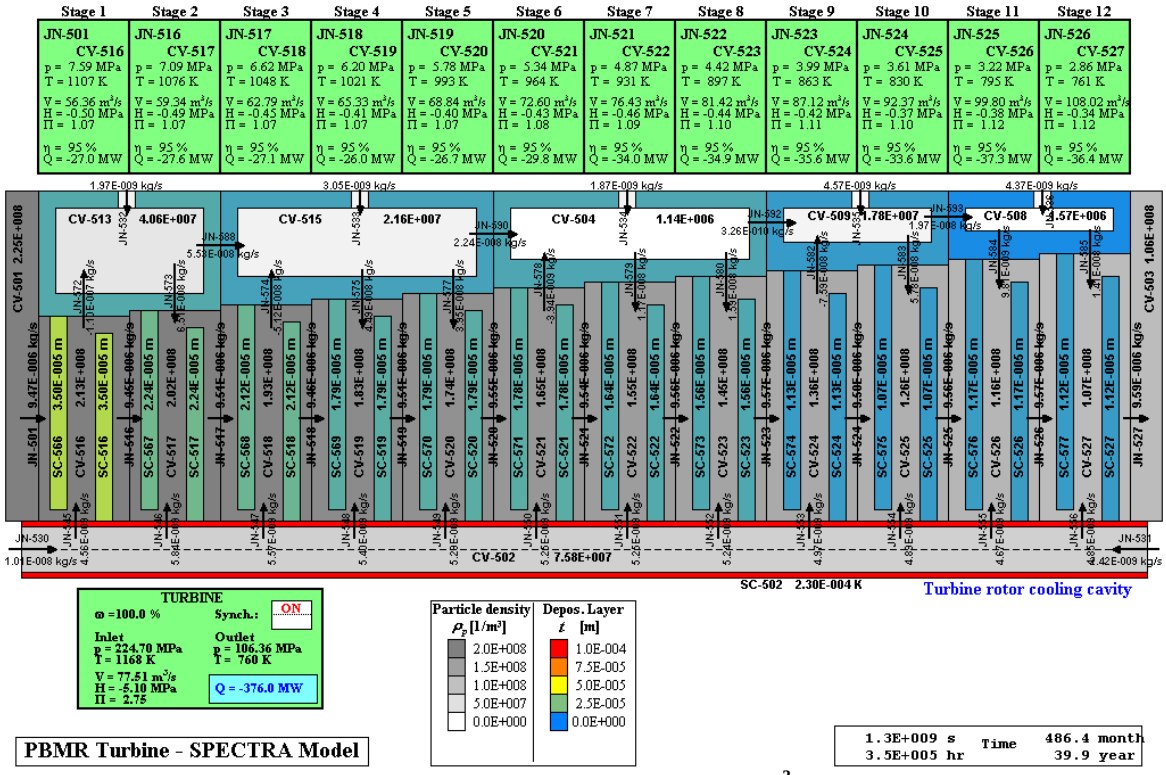

Figure 7 Turbine (stages), airborne dust concentrations [1/m^3] and deposited layer [m]

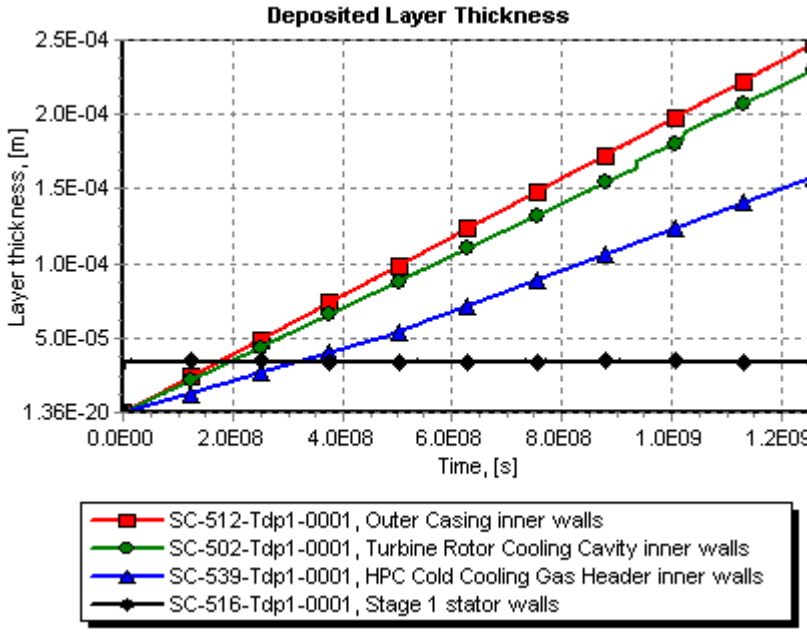

Figure 8 Deposited layer thickness

3.2 Long-Term FP Analysis for the Turbine at 100% Power

The purpose of this run is to investigate fission product transport and deposition (plateout) on the turbine structures during the plant life-time. The plant life-time of 40 years was assumed. Three fission product isotopes were selected for the analysis:

- Cs-137
- I-131
- Ag-110m

These isotopes are of primary importance for the long-term plateout on the metallic surfaces. The fission product concentrations at the turbine boundaries were assumed based on the values calculated for the NGNP plant [7]. This was done in absence of full model PBMR results. The concentrations at the outlet of the NGNP reactor vessel (CV-510) were used. The isotope masses were obtained in a few trial and error runs, to match the vapor pressures in the NGNP outlet pipe are listed in Table 3.

Table 3 Fission product concentrations at the turbine boundaries

Isotope	Vapor No.	Pressure, [Pa] (NGNP)	Mass, [kg]
Cs-137	2	5.0E-09	6.78E-13
I-131	4	5.0E-11	6.49E-15
Ag-110m	12	7.0E-09	7.62E-13

The values listed in Table 3 were used at the turbine inlet (CV-008). The fission product concentrations in the LPC, HPC, and CIP were assumed to be zero. This is a good approximation because the isotopes leaving the turbine will be practically completely adsorbed on the recuperator and the pre-cooler so the concentrations in the LPC, HPC, and CIP are very small. A more detailed numbers should be obtained in the future.

Results for Cs-137, I-131, and Ag-110m, are given in sections 3.2.1, 3.2.2, and 3.2.3, respectively.

3.2.1 Cesium, Cs-137

Results are shown in Figure 9, Figure 10, and Figure 11. The figures show:

- Vapor pressures of cesium in Control Volumes in [Pa], shown using the grey scale.
- Concentrations of fission products adsorbed on metallic surfaces of Solid Heat Conductors in [$1/m^2$], shown using the triple, blue-yellow-red, color scale.

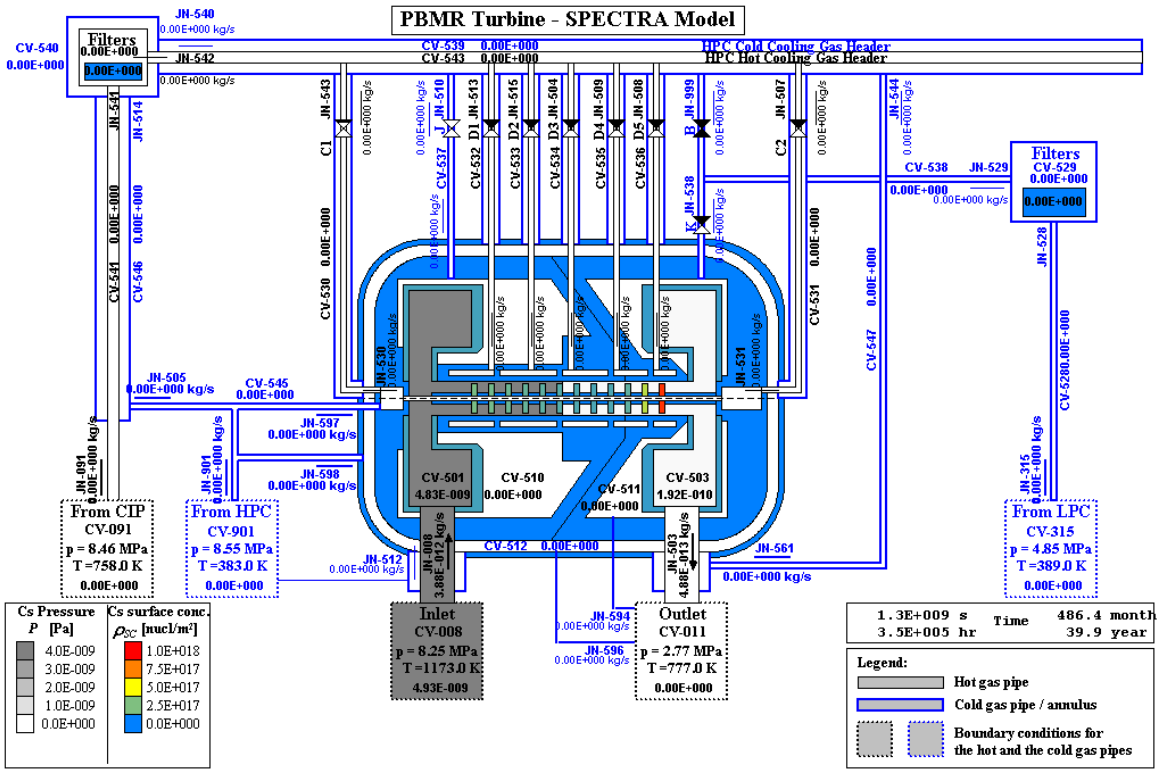

Figure 9Turbine (connections), Cs vapor pressures [Pa] and surface concentrations [1/m^2]

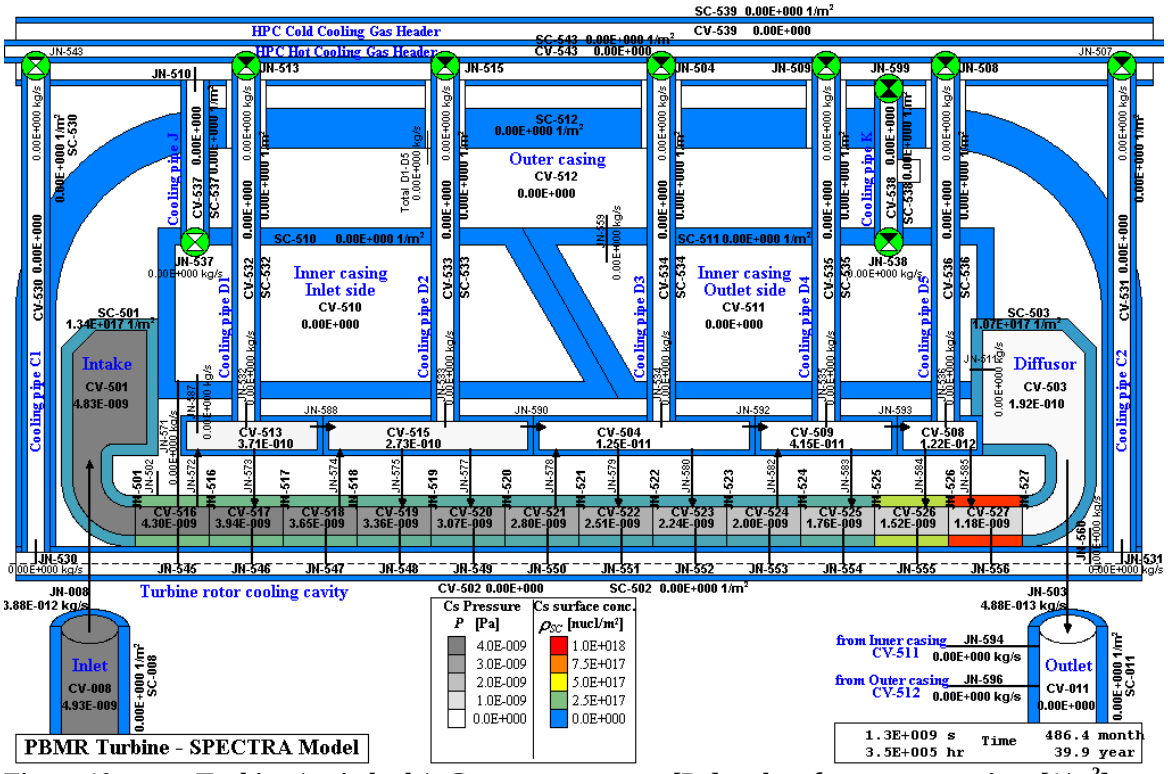

Figure 10 Turbine (main body), Cs vapor pressures [Pa] and surface concentrations [1/m^2]

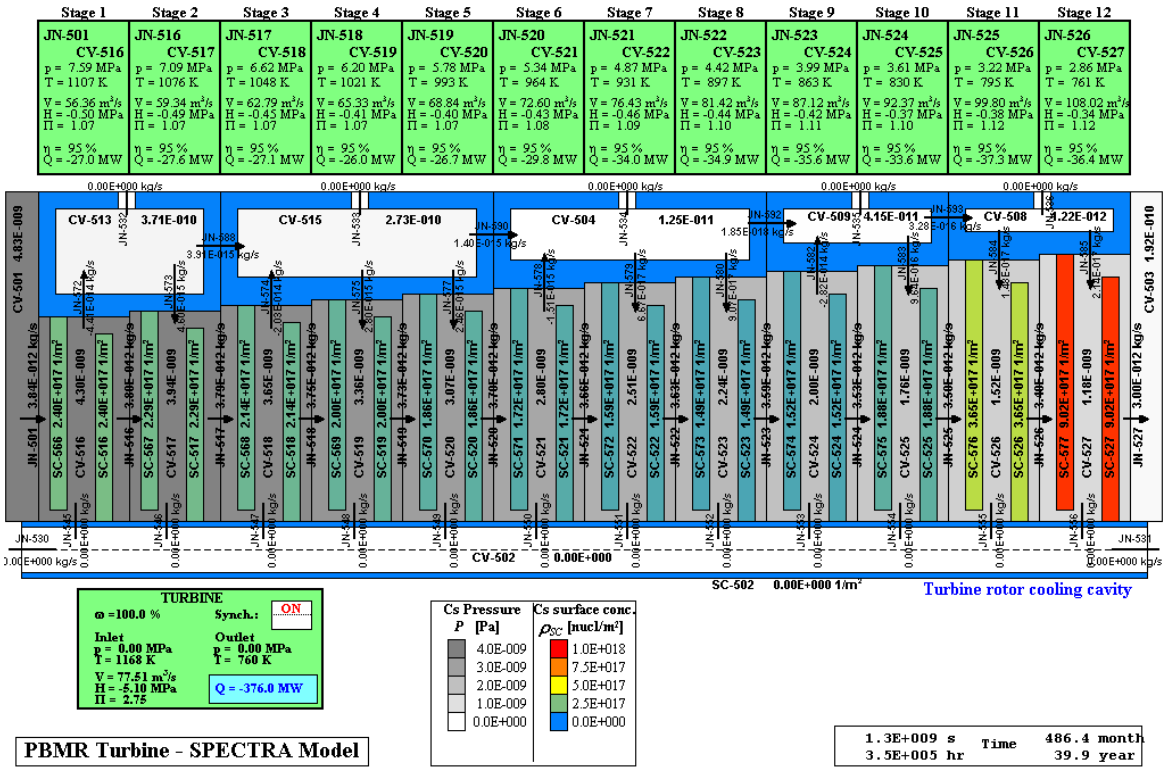

Figure 11 Turbine (stages), Cs vapor pressures [Pa] and surface concentrations [1/m^2]

The incoming flow of Cs-137 is 3.88×10^{-12} kg/s (Figure 10). The mass flow exiting the turbine is 4.88×10^{-13} kg/s (Figure 10). This means that 87% of cesium is adsorbed on the metallic structures of the turbine. The highest concentrations of the adsorbed material is observed in the last stage of the turbine (9.02×10^{17} atoms/m^2 - Figure 11). The high sorption rate in this region is caused by relatively low temperature.

3.2.2 Iodine, I-131

Results are shown in Figure 12, Figure 13, and Figure 14. The figures show:

- Vapor pressures of cesium in Control Volumes in [Pa], shown using the grey scale.
- Concentrations of fission products adsorbed on metallic surfaces of Solid Heat Conductors in [1/m^2], shown using the triple, blue-yellow-red, color scale.

The incoming flow of I-131 is 3.71×10^{-14} kg/s (Figure 13). The mass flow exiting the turbine is 2.23×10^{-14} kg/s (Figure 13). This means that 40% of iodine is adsorbed on the metallic structures of the turbine. The highest concentrations of the adsorbed material is observed in the last stage of the turbine (3.75×10^{12} atoms/m^2 - Figure 14). The high sorption rate in this region is caused by relatively low temperature.

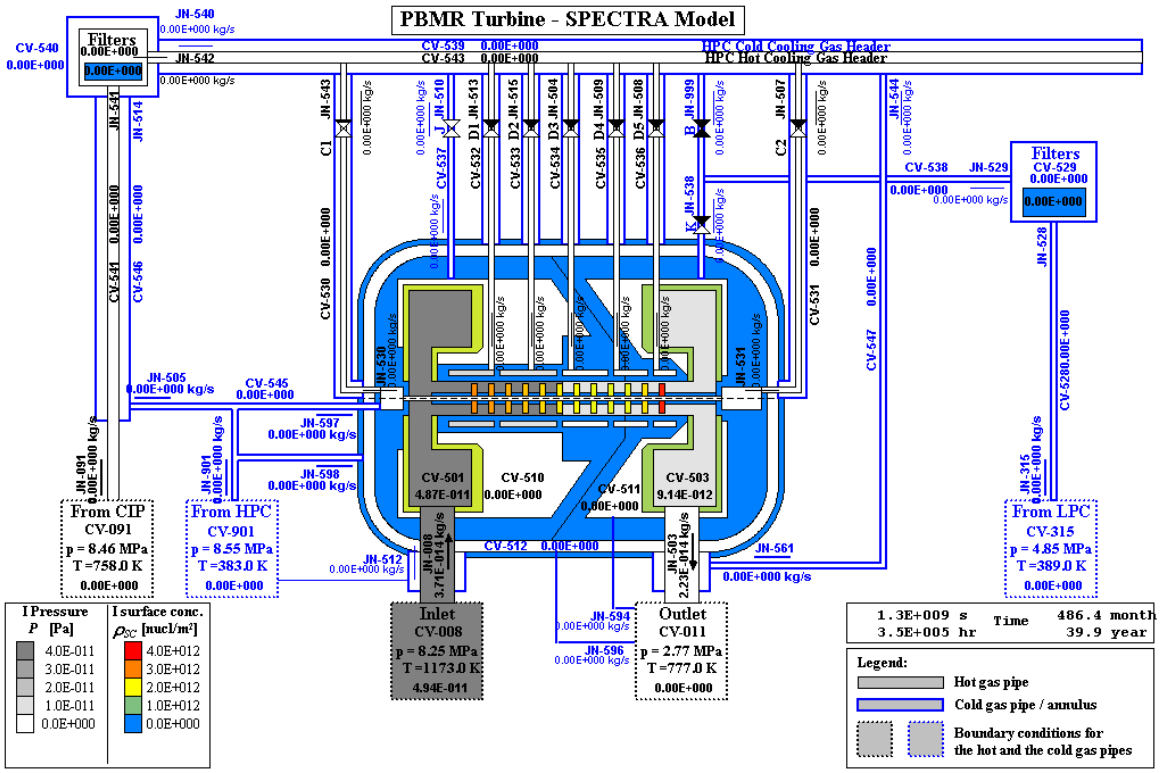

Figure 12 Turbine (connections), I vapor pressures [Pa] and surface concentrations [1/m^2]

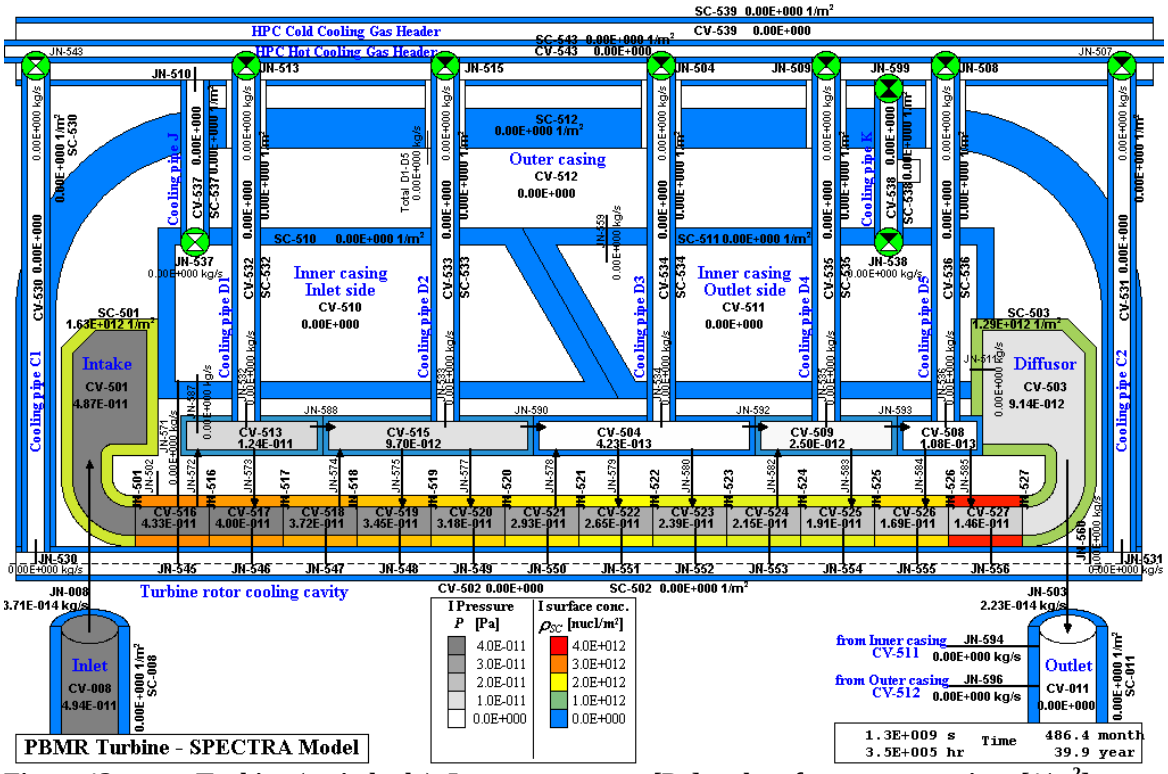

Figure 13 Turbine (main body), I vapor pressures [Pa] and surface concentrations [1/m^2]

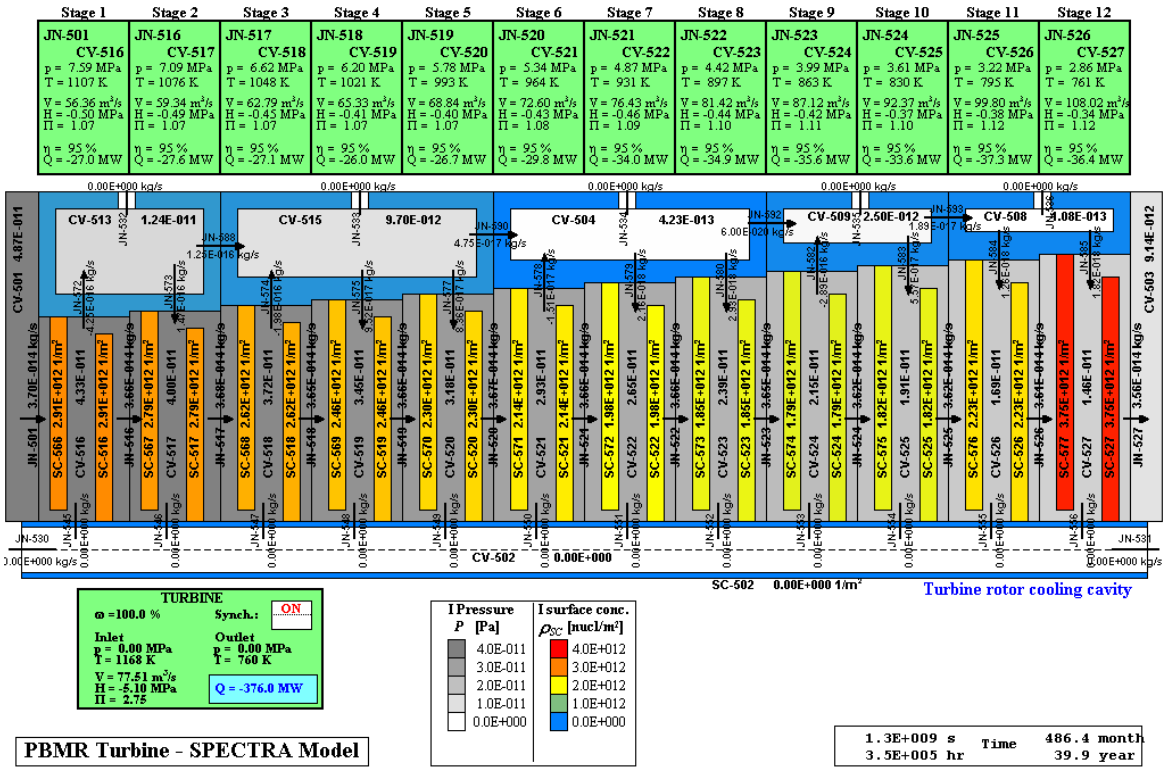

Figure 14 Turbine (stages), I vapor pressures [Pa] and surface concentrations [1/m^2]

3.2.3 Silver, Ag-110m

Results are shown in Figure 15, Figure 16, and Figure 17. The figures show:

- Vapor pressures of cesium in Control Volumes in [Pa], shown using the grey scale.
- Concentrations of fission products adsorbed on metallic surfaces of Solid Heat Conductors in [1/m^2], shown using the triple, blue-yellow-red, color scale.

The incoming flow of Ag-110m is 4.36×10^{-12} kg/s (Figure 16). The mass flow exiting the turbine is 5.21×10^{-15} kg/s (Figure 16). This means that 99.9% of silver is adsorbed on the metallic structures of the turbine. The highest concentrations of the adsorbed material is observed in the stage 10 of the turbine (7.15×10^{17} atoms/m^2 - Figure 17). As in the cases of cesium and iodine, the sorption rate increases along the turbine due to decreasing temperatures. However in the present case the sorption is so large that silver vapor is significantly depleted in the last stages of the turbine. The vapor pressure of silver is 6.01×10^{-9} Pa at in the first stage, 2.47×10^{-9} Pa at in the stage 10, and only 1.09×10^{-11} Pa in the stage 12 (Figure 17). This is a reason for having a maximum in silver concentration in the stage 10.

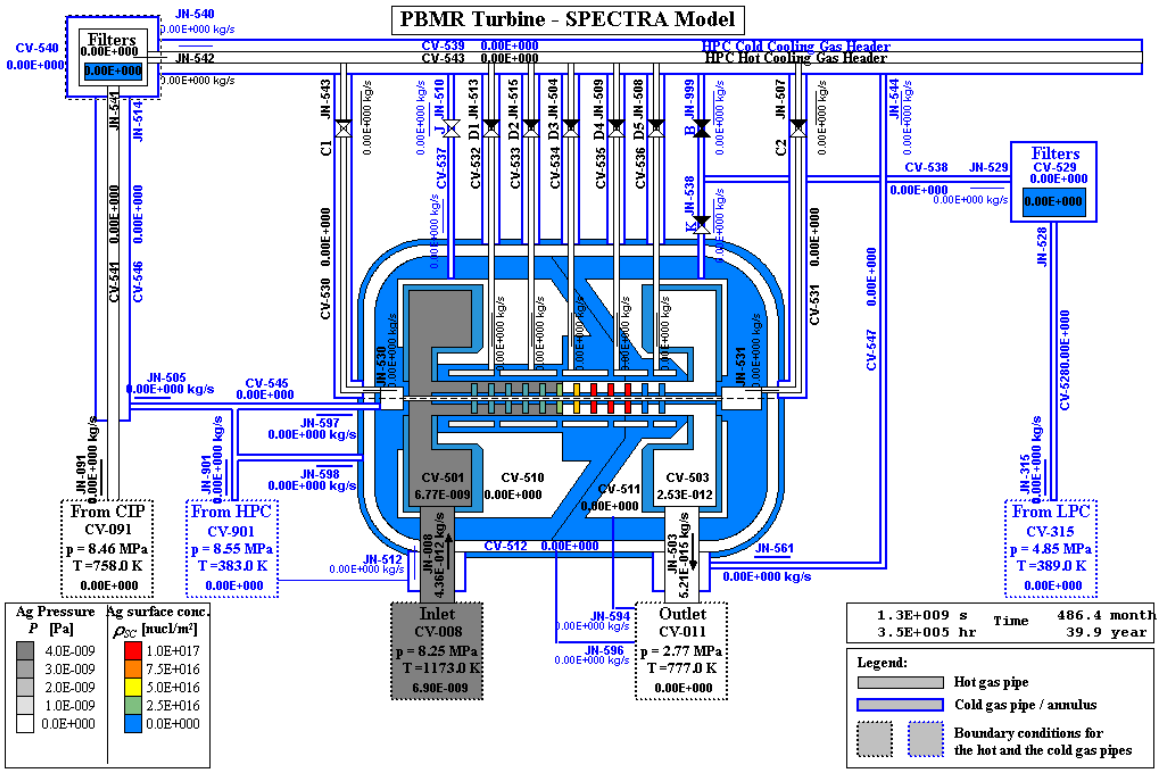

Figure 15 Turbine (connections), Ag vapor pressures [Pa] and surface concentrations [1/m^2]

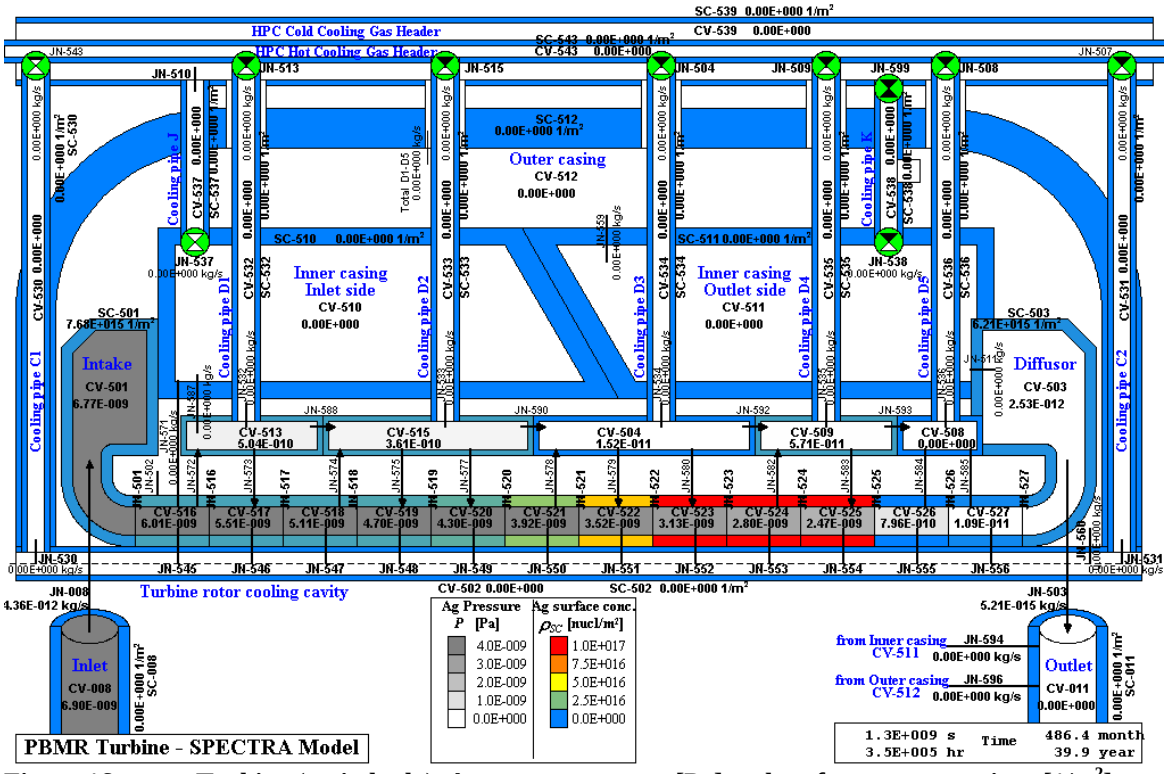

Figure 16 Turbine (main body), Ag vapor pressures [Pa] and surface concentrations [1/m^2]

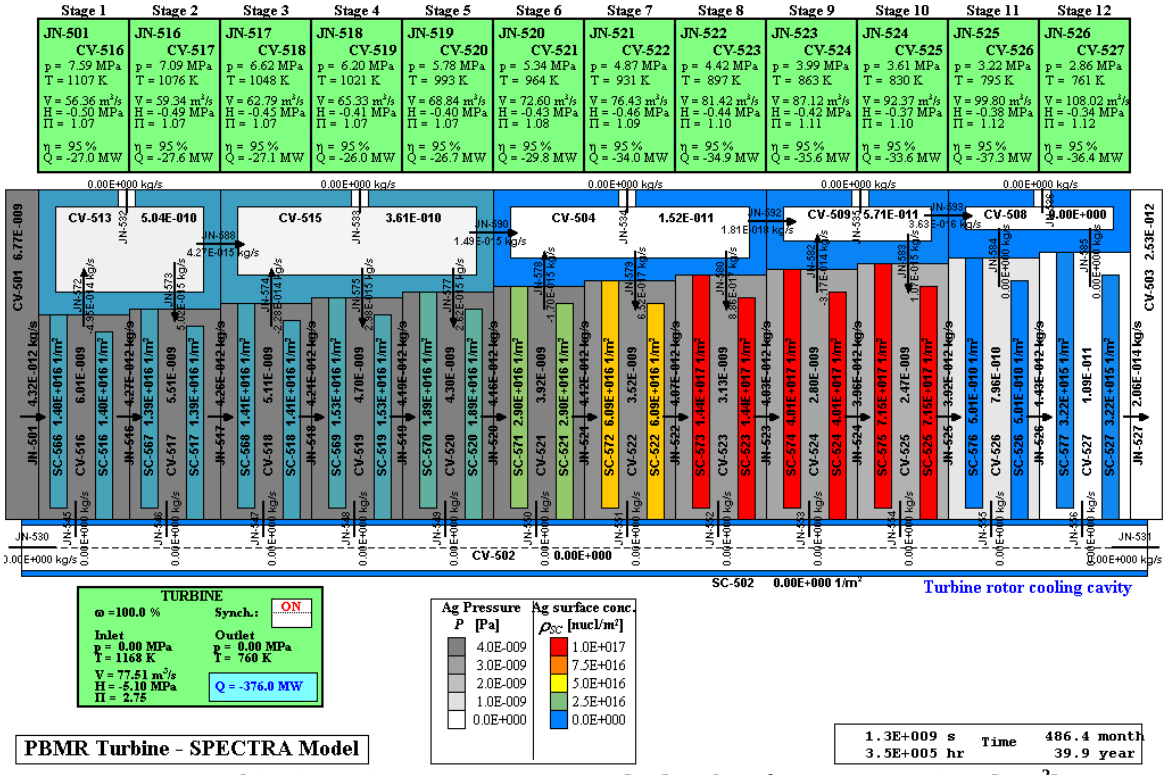

Figure 17 Turbine (stages), Ag vapor pressures [Pa] and surface concentrations [1/m^2]

4 CONCLUSIONS AND RECOMMENDATIONS

This paper presents results of dust and fission product analyses performed for the of the PBMR turbine. The purpose of the present work was to estimate the amount and distribution of deposited dust and the fission products, namely cesium, iodine, and silver, during plant life-time, which was assumed to be 40 full-power years. The turbine design considered here was that which had been designed for the PBMR plant in the year 2008, just before a decision was made not to continue with the PBMR project. The results presented here are of course applicable to this type of turbine its technical parameters, such as filter efficiency etc. If a plant similar to PBMR will be considered in the future the current results and conclusions may not be adequate due to differences in design, operating conditions, etc. The specific conclusions are given below.

4.1 Dust Transport and Deposition

After 40 years of plant life-time deposited layers are very small (of order of 10^{-5} m on the stator and rotor blades - Figure 7). The largest deposition is of course observed on the dust filters (Figure 5). Apart from the dust filters, the largest dust deposition is observed on the:

- Outer Casing (inner walls)
- Turbine Rotor Cooling Cavity (inner walls)
- HPC Cold Cooling Gas Header (inner walls)

This is caused by relatively low gas velocities in these volumes. These low velocities allow a continuous build-up of the dust layer. In other places of the system the dust is resuspended very quickly due to large gas velocities, and an equilibrium layer develops. The equilibrium layer thickness is a result of coagulation of the deposited dust; as the larger particles are quickly resuspended. Therefore the net deposition of dust on the turbine structures is relatively small, i.e. practically all dust entering the turbine intake is passing through to the turbine outlet.

4.2 Fission Product Transport and Plateout

In the present analysis the fission product concentrations in the LPC, HPC, and CIP were assumed to be zero. This is a good approximation because the isotopes leaving the turbine will be practically completely adsorbed on the recuperator and the pre-cooler so the concentrations in the LPC, HPC, and CIP are very small. A more detailed numbers should be obtained in the future.

About 90% of cesium, 40% of iodine, and 99.9% of silver is adsorbed on the metallic structures of the turbine. The sorption rate increases along the turbine due to decreasing temperatures. In case of cesium and iodine the highest concentrations are observed in the last stage (stage 12) of the turbine. In the case of silver the sorption is so large that silver vapor is significantly depleted in the last stages of the turbine. This is a reason for having a maximum in silver concentration in the stage 10. In the following stages the concentration decreases due to very small silver vapor fraction in the gas.

Nomenclature

Symbols

$A(T)$, $B(T)$	temperature-dependent sorption coefficients
C_d	isotope concentration on the surface [kg/m^2]
$C_{\max}$	maximum number of sorption sites per unit surface area, [m^{-2}]
C_{rev}	number of adsorption sites occupied by reversibly bound molecules per unit surface area, [m^{-2}]
C_V	isotope concentration in the gas volume, [kg/m^3]
C_δ	vapor concentration in the δ-sublayer, [kg/m^3]
S_{total}	total sorption flux, [kg/s]
S_{diff}	part of the sorption flux that penetrates and diffuses into the material, [kg/s]
T_w	wall temperature, [K]

Greek symbols

α	sticking coefficient, [-]
$(1-\beta)$	penetration factor, [-]
η	evaporation coefficient, [s^{-1}]
ϑ	desorption coefficient, [s^{-1}]
θ	reversible surface coverage, [-]

Abbreviations

CIP	Core Inlet Pipe
CV	Control Volume
HPC	High Pressure Compressor
JN	Junction
LPC	Low Pressure Compressor
SC	1-D Solid Heat Conductor
RT	Radioactive Particle Transport Package in SPECTRA

References

[1] M.M. Stempniewicz, "SPECTRA - Sophisticated Plant Evaluation Code for Thermal-hydraulic Response Assessment, Version 3.60, April 2010, Volume 1 - Program Description; Volume 2 - User's Guide; Volume 3 - Subroutine Description; Volume 4 - Verification", NRG report K5024/10.101640, Arnhem, April 2010.

[2] Gas Path Design, PBMR-MHI-116 R-1.

[3] PBMR Turbine, Mitsubishi Heavy Industry (MHI) Model, Nodalization Diagram.

[4] PBMR Turbine, Flownex Model, Nodalization Diagram.

[5] Turbine pressures, temperatures and mass flow data - various sources available at PBMR

[6] M.M. Stempniewicz, "PBMR Turbine Model for SPECTRA Dust and Plateout Analyses", NRG note 912164/09.97283 S&P/MST, August 2009.

[7] M.M. Stempniewicz, L. Winters, S.A. Caspersson, "Analysis of dust and fission products in a pebble bed NGNP", *Nuclear Engineering and Design* **251** (2012) 433– 442

[8] M.M. Stempniewicz, "Sorption Coefficients for Iodice, Silver, and Cesium on Dust Particles", NRG note 912164/09.97104 S&P/MSt Rev. 1, August 2009.

[9] L. Stassen, "RADAX4, Validation Test Report", PBMR Document No. 026638, Revision 1, September 22, 2005.

[10] R.O. Gauntt, et.al., "MELCOR Computer Code Manuals, Version 1.8.6, September 2005", NUREG/CR-6119, Vol. 1, 2, Rev. 3, SAND 2005-5713, published: September 2005.

[11] T. S. Kress, F. H. Neill, "A Model for Fission Product Transport and Deposition under Isothermal Conditions", ORNL-TM-1274, 1965.

[12] N. Iniotakis, „Rechenprogramm PATRAS, Programmbeschreibung", KFA IRB-IB-7/84, Research Center Jülich, 1984.